



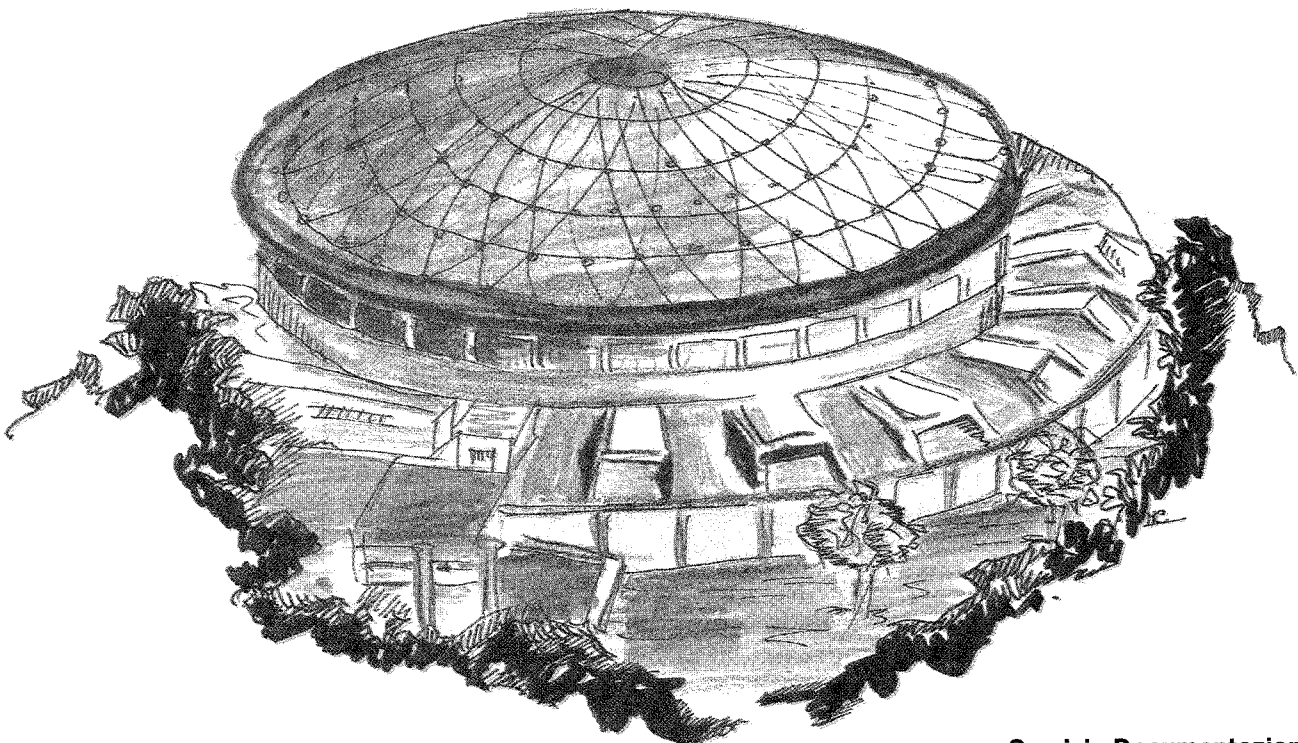
Laboratori Nazionali di Frascati

Submitted to Nucl. Instr. & Meth. in Physics Res.

LNF-90/082(P)
31 Ottobre 1990

M. Castellano, A. Ghigo, P. Patteri, C. Sanelli, M. Serio, F. Tazzioli, N. Cavallo,
F. Cevenini, F. Ciocci, G. Dattoli, A. Dipace, G.P. Gallerano, A. Renieri, E. Sabia,
A. Torre:

STATUS REPORT OF THE IR FEL PROJECT ON THE SC LINAC LISA AT LNF-FRASCATI



INFN - Laboratori Nazionali di Frascati
Servizio Documentazione

LNF-90/082(P)
31 Ottobre 1990

STATUS REPORT OF THE IR FEL PROJECT ON THE SC LINAC LISA AT LNF-FRASCATI

M. Castellano, A. Ghigo, P. Patteri, C. Sanelli, M. Serio, F. Tazzioli

INFN-LNF, C.P. 13, 00044 Frascati (Rome), Italy

N. Cavallo, F. Cevenini

INFN-Sezione di Napoli and Univ. di Napoli-Dipart. di Scienze Fisiche, Napoli, Italy

F. Ciocci, G. Dattoli, A. Dipace, G.P. Gallerano, A. Renieri, E. Sabia, A. Torre

ENEA-CRE Frascati, 0044 Frascati (Rome), Italy

ABSTRACT

We report the progress of the superconducting linac LISA at LNF (Frascati National Laboratories) and the status of the FEL experiment. The design of the optical cavity is presented.

1. INTRODUCTION

The LISA project was approved and funded by INFN at the end of 1987 as a small pilot facility in the framework of a long term R&D program on superconducting linear accelerators [1]. An infrared FEL experiment in collaboration with the ENEA-TIB department was also approved with the aim of testing and exploiting the high quality beam provided by the SC linac and to continue the research line on FEL's in which LNF has been involved since 1980. In June 1990 INFN funded further R&D activity and approved the ARES project, a program to build a 240 MeV SC linac, developing the technology of high field SC cavities in collaboration with Italian industry [2]. The LISA accelerator and its ancillary buildings will become part of the new complex. Although this requires no major changes of the present experimental program, some modifications have been carried out in the linac output transport line to make it more compatible with future activities and to minimize the overall engineering effort on the whole project. The parameters of the LISA beam and of the FEL are listed in tab. I.

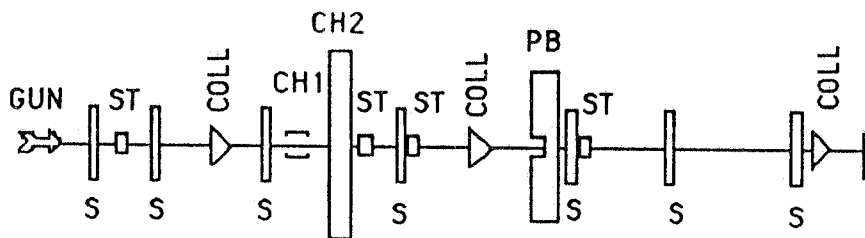
Table I - Parameter list of the LISA accelerator and FEL.

<i>Energy</i>	25	<i>MeV</i>
<i>Bunch length</i>	2.5	<i>mm</i>
<i>Peak current</i>	5	<i>A</i>
<i>Duty cycle</i>	≤ 10	<i>%</i>
<i>Average macropulse current</i>	2	<i>mA</i>
<i>Invariant emittance</i>	10^{-5}	$\pi m \cdot rad$
<i>Energy spread (@25 MeV)</i>	$2 \cdot 10^{-3}$	
<i>Micropulse frequency</i>	50	<i>MHz</i>
<i>Macropulse frequency</i>	10	<i>Hz</i>
<i>Undulator periods N</i>	50	
<i>Undulator wavelength</i>	4.4	<i>cm</i>
<i>Undulator parameter K_{rms}</i>	$0.5 \div 1.0$	
<i>Radiation wavelength @ 25 MeV</i>	$11 \div 18$	μm
<i>Linewidth @ 15 μm</i>	0.5	<i>%</i>
<i>Small signal gain @ 15 μm</i>	17.3	<i>%</i>
<i>Small signal gain @ 5 μm (3rd harmonic)</i>	2.5	<i>%</i>

2. MACHINE CONSTRUCTION PROGRESS

LISA consists of a 1 *MeV* injector and four 4-cell SC cavities, each of four cells, with an average accelerating gradient of 5 *MV/m*, providing a 25 *MeV* beam with emittance $\epsilon \approx 2 \cdot 10^{-7}$ and peak current $\approx 5 A$.

The schematics of the injector [3] is shown in fig. 1. All elements have been built and separately tested [4,5,6]. The design specs and present performance are given in tab. II.



S - Solenoidal lenses; ST - Steerings; COLL - Collimator; CH1 - Chopper 1 (50MHz); CH2 - Chopper 2 (500MHz); PB - Prebuncher (500MHz).

FIG. 1 - Sketch of the injector line at 100 kV.

Table II - Design specs and present performance of the LISA injector components.

<i>Component performance</i>	<i>design</i>	<i>achieved</i>
Gun		
Macropulse charge [μC]	400	320
Emittance [$\text{m} \cdot \text{rad}$]	$1 \cdot 10^{-5}$	$1 \cdot 10^{-5}$ (@ 100 mA)
Gun power supply		
Voltage [kV]	100	100
Current [mA]	200	160
Chopper 50 MHz [W]	90	250
Chopper 500 MHz [kW]	1.2	1.3
Prebuncher 500 MHz [W]	260	300
1 MeV capture section 2.5 GHz [kW]	20	20

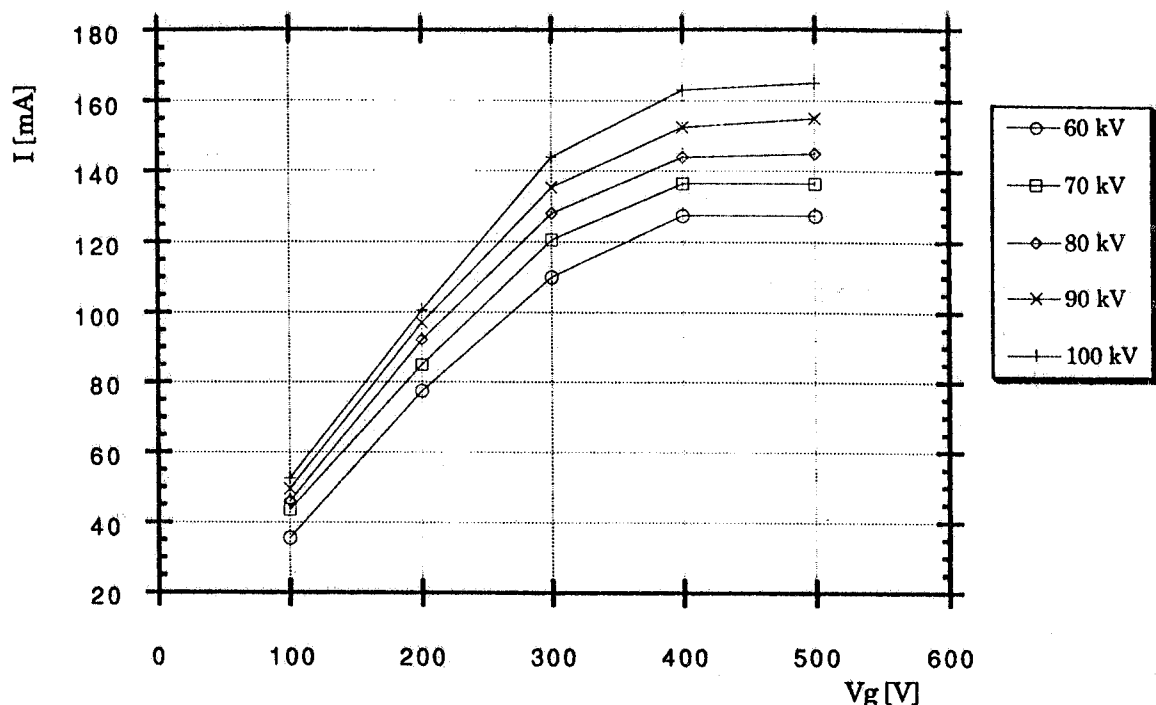


FIG. 2 - Gun current vs. grid voltage as a function of the accelerating potential.

Extensive tests of the gun are being carried on in this stage because the final assembly will prevent a direct measurement of its performances.

The LISA duty cycle is specified to be 2% in routine operation with long macropulses. Higher duty cycle will be possible with different pulse structures or in the energy recovery mode subject to the restriction that the beam power loss in the beam dumper does not exceed 1 kW. In order to exploit the high d.c. capability of SC linacs the gun power supply has been designed to provide a

continuous d.c. voltage of 100 kV @ 200 mA .

The characteristic gun current vs. grid voltage curves are shown in fig. 2.

The saturation current ($\approx 160\text{ mA}$) is at present lower than the nominal value ($\approx 200\text{ mA}$) because of insufficient cathode heating. The measured perveance is $6 \cdot 10^{-6}\text{ AV}^{-3/2}$, in good agreement with the design value.

The experimental layout for the gun emittance measurement is shown in fig. 3.

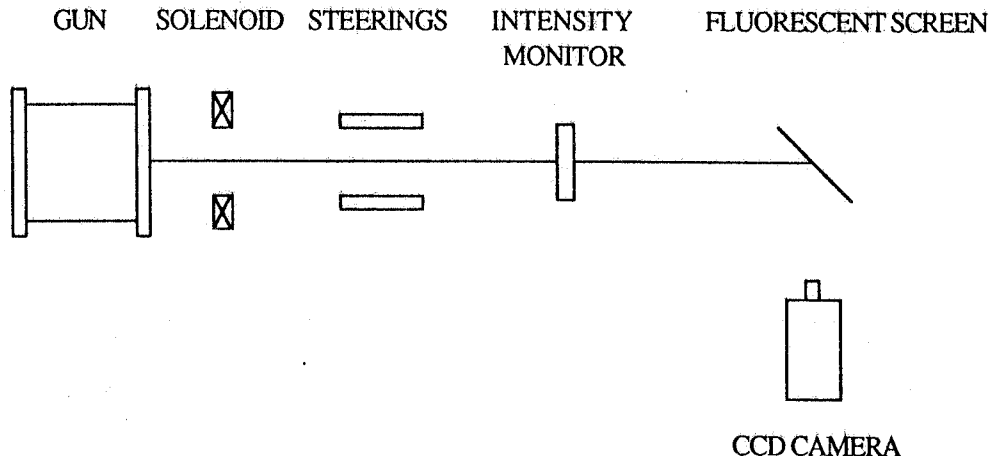


FIG. 3 - Layout of the experimental set-up for emittance measurement.

A gated CCD TV camera and a frame grabber are used to obtain a picture of the beam spot on a 45° fluorescent ceramic target (see fig. 4). The pressure rise caused by sputtering when the target is hit by the beam can be harmful to the cathode emitting surface; low repetition rates ($\approx 0.5\text{ Hz}$) are therefore used during this measurement. Because the decay time constant of the fluorescence is $\approx 10\text{ ms}$, a useful image lasts only one TV frame; a synchronization system is therefore required to get the picture in the first frame after the beam pulse. The digitized frame is stored on mass memory for off-line analysis.

Although the beam behaviour is reproducible, the best beam shape has not yet been obtained at the maximum transmitted current. Since the anode shape is optimized to counteract the space charge force at the nominal current of 200 mA , the size of the extracted beam is somewhat larger at lower currents. This makes the beam shape more sensitive to stray and nonlinear magnetic fields along its path. Full rating commissioning and conditioning of the gun will be completed after upgrading the cathode heater supply and improving the stray field screening.

Nevertheless preliminary analysis of the beam spot measurements has been carried out at 90 kV and 100 mA giving a normalized rms emittance $\approx 10^{-5}\text{ m} \cdot \text{rad}$.

The RF tests of the chopper and prebuncher cavities have been completed [4]. The 1 MeV capture section has been tested and conditioned at full RF power without beam [5]. The magnetic measurements and the assembly of the elements of the transport line from the injector to the SC linac is in progress. The test of the completely assembled injector will have to be carried out in the

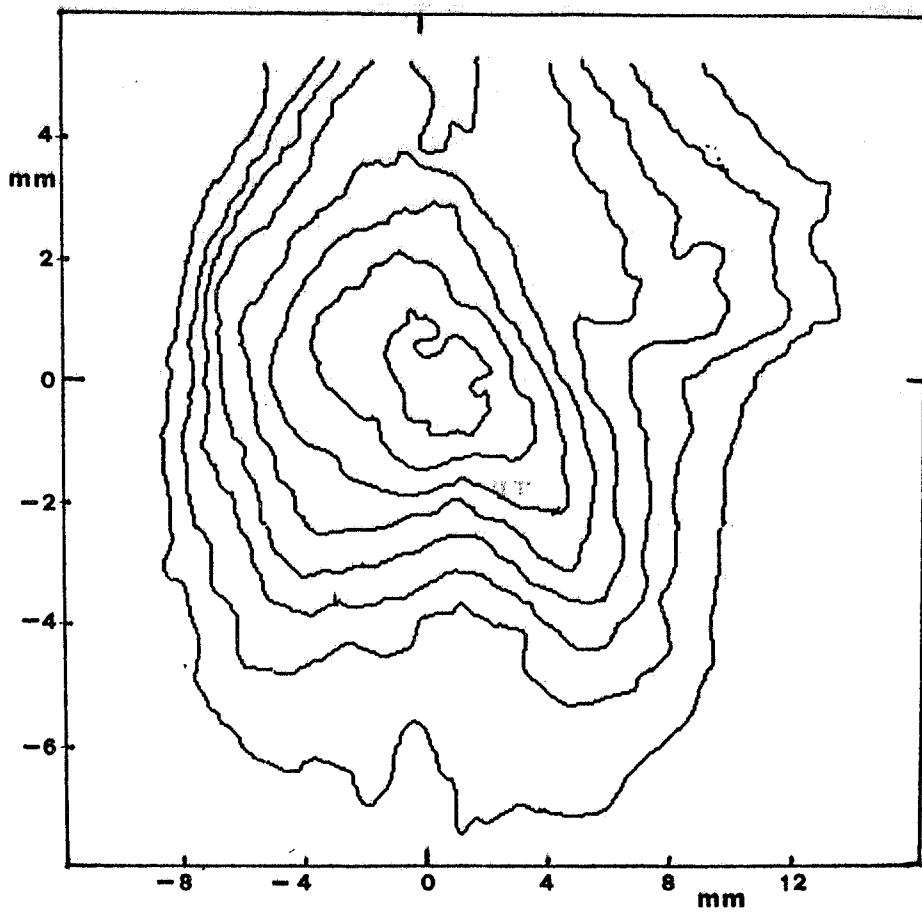


FIG. 4 - Contour plot of a beam spot at 90 kV and 100 mA, obtained from a TV picture.

final underground hall, that will be available before the end of Sept. 1990, because of the radiation shielding requirements. Only partial tests in temporary locations have therefore carried out in the meantime. The tests also served to check some of the most relevant parts of the final diagnostics and control system [7].

Cold tests of the main linac cavities started at the manufacturing industry (Interatom). The delivery of all four cavities is foreseen within the end of this year.

The 25 MeV transport line from the linac to the undulator has been redesigned to reduce the number of different magnetic elements. In the new lattice quadrupoles identical to those used in the 1 MeV injection arc are used. Moreover, standard bending magnets with $\rho = 0.5 \text{ m}$ and $\phi = 30^\circ, \text{m}$ that can reach up to 250 MeV, are used. The arc lattice includes 6 bending magnets, arranged in 3 achromatic doublets. It is not isochronous but its dispersion causes a pulse lengthening of only 5% at the nominal energy spread. On the other side the dispersion-free sections between doublets ensure simple beam control. The FEL undulator is positioned immediately downstream from the last magnet of the arc.

3. FEL PROGRESS

The undulator has been studied and designed in collaboration by ENEA and ANSALDO [8]. The construction is in progress at ANSALDO. Its completion is foreseen by the end of this year.

The undulator length is $l_u = 2.2 \text{ m}$; to provide space for the lattice and to accomodate steering and focusing elements the cavity length l_c has to be $> 5 \text{ m}$. The synchronism condition between the 20 ns spaced electron bunches and the photon round trip time inside the cavity fixes the shortest symmetric cavity length at $l_c = 6 \text{ m}$.

A simplified model of the FEL interaction gives for the optimal Rayleigh length Z_0 a value in between $l_u/2$ and $l_u/2\sqrt{3}$. The former corresponds to a confocal configuration minimizing diffraction losses due to undulator gap, the latter is obtained by maximizing the integral of the laser intensity along the undulator [9]. Following the analysis of the laser- e^- beam interaction carried out in ref. [10] and including the beam emittance effect, the relative FEL gain turns out to be nearly constant over this range. Owing to the low emittance, the transverse beam size is smaller than the optical mode in the fundamental harmonic and comparable to it in third harmonic operation. The configuration with the largest Rayleigh length was finally selected because it is less sensitive to beam emittance effects [11].

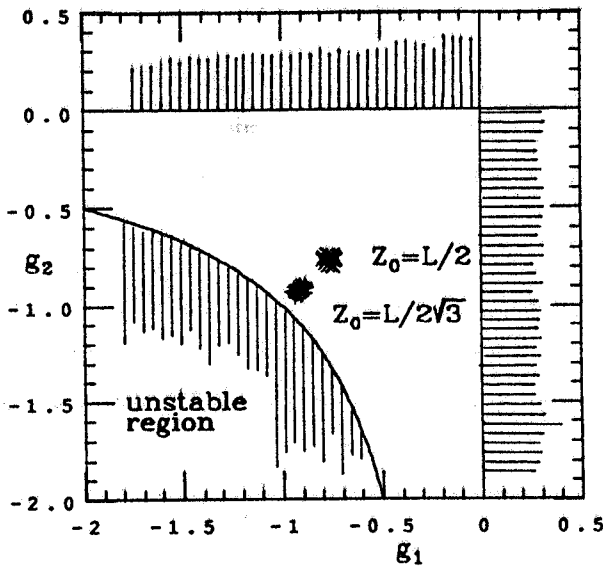


FIG. 5 - Spreading of the optical cavity representative points on the stability diagram at $g = -0.765$ and $g = -0.914$ showing the effect due to 2% error of mirror radius.

Moreover, a larger Z_0 is preferable when alignment and mirror radius errors are taken into account. The mirror curvature radius at a distance z from the waist is given by

$$R(z) = z \left(1 + (Z_0/z)^2 \right)$$

At $z = 3 \text{ m}$ the radius is $R = 3.40 \text{ m}$ corresponding to a stability parameter $g = 1 - d/R = -.765$. The spreading of this parameter, when a curvature error of 2% is assumed, is shown in fig. 5. For comparison the points corresponding to a cavity with $Z_0 = l_u/2\sqrt{3}$ with the same error distribution are also shown. In the latter case $R = 3.14 \text{ m}$ and $g = -0.914$ giving a quasi concentric cavity, near the instability border. The design parameters of the cavity are listed in tab. III.

Table III - Parameter list of the optical cavity.

<i>Length L_c</i>	6	m
<i>Rayleigh length Z_0</i>	1.1	m
<i>Mirror radius R</i>	3.40	m
<i>1st harmonic</i>	15	μm
<i>Waist w_0</i>	2.3	mm
<i>Spot size on mirrors</i>	6.7	mm
<i>Cavity losses</i>	1	%
<i>Output coupling</i>	1	%
<i>Peak power</i>	1.2	MW
<i>Macropulse averaged power</i>	500	W
<i>Average power</i>	50	W
<i>3rd harmonic</i>	5	μm
<i>Waist w_0</i>	1.3	mm
<i>Spot size on mirrors</i>	3.8	mm

The mechanics of the cavity end pieces has been defined. The pivoting arms of the mirror holders are in air, actuated by external piezoelectric pushers (PZT), to avoid the complication of micrometric movements in vacuum. The effect of the atmospheric pressure force on the flexible joint of the mirror holder is cancelled by the force on a similar joint between the holder and the exit window flange. The mirror holder is spring loaded to ensure a proper contact with the PZT end cups. The mechanical drawing of the device mounted on the slider for longitudinal tuning is shown in fig. 6.

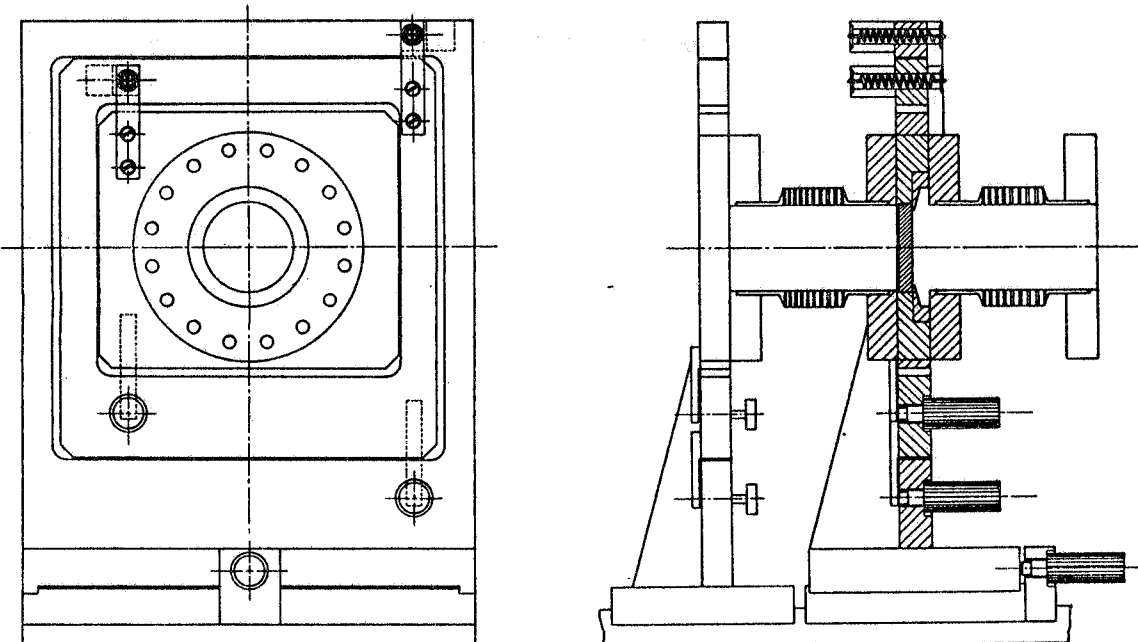


FIG. 6 - Mechanical drawing of the optical cavity head, with the longitudinal tuning movement and the transverse tuning actuators.

The pivoting arms are 110 mm long and the PZT lengthening is 25 μm . The mirror tilting is $\pm 115 \mu\text{rad}$, providing a parallel displacement of the cavity axis of $\pm 0.4 \text{ mm}$ and a tilting of $\pm 1 \text{ mrad}$. Mechanical prealignment of the optical cavity can be realized with errors in this range, corresponding to a just-overlapping alignment.

REFERENCES

- [1] A. Aragona et al., 'The Linear Superconducting Accelerator Project LISA', in Proceedings of European Particle Accelerator Conference, p. 52, Rome 1988
- [2] 'The ARES Superconducting Linac' - Report LNF-90/035(R), Frascati, May 1990
- [3] A. Aragona et al., 'Injector for LISA', in 1988 Linear Accelerator Conference Proceedings, p. 400, CEBAF Report 89-001
- [4] R. Boni et al., 'The RF System of Frascati LISA 1 MeV Injector' to appear in Proceedings of 1990 European Particle Accelerator Conference.
- [5] A. Aragona et al., '1 MeV Capture Section for LISA Injector', to appear in Proceedings of 1990 European Particle Accelerator Conference.
- [6] A. Aragona et al., 'The Injector of the Superconducting Linac LISA', to appear in Proceedings of 1990 Linear Accelerator Conference.
- [7] M. Castellano et al., 'Computer control and diagnostic equipment for the LISA project', to appear in Proceedings of 1990 European Particle Accelerator Conference.
- [8] L. Barbagelata et al., 'Advanced concepts in mechanical design and computerized control system for a hybrid permanent magnet undulator', to appear in Proceedings of the 12th FEL Conference, Paris 1990.
- [9] R. Barbini, G. Vignola, Internal report LNF-80/12/(R)
- [10] B. W. Colson, P. Elleaume, Appl. Phys. B29, 101 (1982)
- [11] P. Patteri, 'Design considerations on the optical cavity for SURF', Adone Int. Memo LIS-77